not available, but the present level of theory is expected to provide a good approximation.

Summary and Conclusions

In the present ab initio studies of adenine and guanine, both the MRCI and RPA calculations have revealed the presence of 20 to 25 singlet–singlet electronic transitions in the spectral region between 35 000 and 55 000 cm^{-1}, a number considerably higher than is predicted by semiempirical calculations. Errors in calculated transition energies obtained with both the MRCI and RPA methods were found on average to fall within a range of 12 000–15 000 cm^{-1}, and linear scalings of calculated transition energies have been used to provide an approximate qualitative resolution of the absorption spectra.

The lowest absorption band of adenine at 38 500 cm^{-1} (band I) is shown by both methods to arise from a group of two $\sigma \rightarrow \pi^*$ and three $\pi \rightarrow \pi^*$ electronic transitions, only one of which is calculated as intense. In guanine, band I at 36 300 cm^{-1} contains two $\pi \rightarrow \pi^*$ transitions, and band II at 40 000 cm^{-1} arises from one $\sigma \rightarrow \pi^*$ and three $\pi \rightarrow \pi^*$ transitions. The calculated polarizations of these bands do not agree with experimental values obtained for crystals. It is clear, however, that the actual polarizations are likely to be very sensitive to changes in molecular environment, and that calculated polarizations are quite sensitive to the level of theory. Therefore, it appears that it is not possible to obtain or assign definite values for the polarizations of the low-energy bands.

In the spectra of both molecules between 45 000 and 55 000 cm^{-1}, a large number of transitions of varying intensity were found in both the MRCI and RPA studies, but the number and characteristics of the constituent transitions found differ between the two methods. Nevertheless, the general features of the broad-banded absorption in this spectral region are described by both methods.

Adenine and guanine each possess several triplet (π,π^*) states which lie lower in energy than the lowest excited singlet state, S_1. In adenine, there are four triplet (π,π^*) states below the lowest excited singlet state, with T_1 predicted to lie only 24 930 cm^{-1} above the ground state, S_0. In guanine, T_1 and T_2 are located at approximately 28 280 and 29 520 cm^{-1} above S_0, respectively, with T_3 and T_4 isoenergetic with S_1.

Thus, it appears that the current ab initio investigation of the spectral properties of adenine and guanine has uncovered a number of subtle features heretofore unrecognized in earlier theoretical studies. Specifically, use of a more extended basis set which includes diffuse functions has, not unexpectedly, given rise to a considerably denser manifold of excited states. And as was shown, the resultant near degeneracy of several transitions in each of the spectral regions of interest leads to an enhanced sensitivity of the calculated polarizations to the level of theory employed. An important consequence of this is that the results of high-level calculations such as those described here may not be sufficient to produce reliable transition density distributions for use in exciton calculations. Furthermore, the spectral congestion revealed in the present study strongly suggests that experimentally determined polarizations of transitions determined for crystals are not expected to be valid in other molecular environments. Thus, both adenine and guanine possess absorption spectra which lack simplicity, in that there are no bands in which the intensity is provided by a single isolated transition, which could be more easily characterized both theoretically and experimentally.

---

(69) DeVoe, H.; Tinoco, I. *J. Mol. Biol.* **1962**, *4*, 500–517.

Computational Studies of Open-Shell Phosphorus Oxyacids. 1. P–H Bond Homolysis in H_2PO_2

Christopher J. Cramer* and George R. Famini

Contribution from the U.S. Army Chemical Research Development and Engineering Center, Research Directorate, Physics Division, Chemometric and Biometric Modeling Branch, Aberdeen Proving Ground, Maryland 21010-5423. *Received February 5, 1990*

Abstract: The hypothetical molecule dihydrodioxophosphoranyl (**1**) has been studied computationally. Both 3-21G$^{(*)}$ and 6-31G* unrestricted Hartree–Fock (UHF) wave functions exhibited inherent doublet instability which was corrected for by consideration of correlation effects. Configuration interaction proved most effective in this respect, while Møller–Plesset perturbational corrections were fair when extended to third order and only marginal when truncated at second order. The barrier to P–H bond homolysis was determined to be 4.8 ± 0.3 kcal/mol. The metastability of **1** has been explained in the formalism of valence bond theory. It arises from interactions of degenerate valence bond functions corresponding to reactants and products with an intermediate configuration corresponding to a $n \rightarrow \pi^*$ ($1A_2 \rightarrow 3B_1$) excited state. Predicted spectral data to aid in the identification of **1** are presented.

Organophosphorus compounds are ubiquitous in nature. Indeed, organophosphate intermediates are involved in nearly all energy transformations in living matter.[1] In the environment, organophosphorus species may be found in many forms, including fertilizers, detergents, and pesticides. The latter class can pose particular environmental problems with respect to long-term contamination.[2] This is especially the case when a compound exhibits significant mammalian neurotoxicity as an acetylcholine esterase inhibitor,[3] and the development of effective detoxification procedures for these compounds has occupied numerous research groups for many years.[4]

A large number of neurotoxic pesticides are organophosphonates, i.e., phosphorus(V) species with a single phosphorus–carbon bond. It has been observed that the microorganism

---

(1) Classical references include: (a) Erecinska, M.; Wilson, D. F. *Trends Biochem. Sci.* **1978**, *3*, 219. (b) Newsholme, E. A.; Start, C. *Regulation in Metabolism*; Wiley: New York, 1973. (c) Kelcker, H. M. *Biological Phosphorylations*; Prentice-Hall: New York, 1969.

(2) (a) Becker, E. L.; Fukoto, T. R.; Boone, B. Canham, D. C.; Boger, E. *Biochemistry* **1963**, *2*, 72. (b) *Organophosphorus Pesticides: Organic and Biological Chemistry*; Eto, M., Ed.; CRC Press: Cleveland, 1974.

(3) Main, R. A.; Iverson, F. *Biochem. J.* **1966**, *100*, 525.

(4) (a) Biresaw, G.; Bunton, C. A.; Quan, C.; Yang, Z.-Y. *J. Am. Chem. Soc.* **1984**, *106*, 7178. (b) Bunton, C. A.; Mhala, M. M.; Moffatt, J. R.; Monarres, D.; Savelli, G. *J. Org. Chem.* **1984**, *49*, 426. (c) Moss, R. A.; Swarup, S. *Tetrahedron Lett.* **1984**, 4079. (d) Rutkovskii, G. V.; Begunov, A. V.; Kuznetsov, S. G. *J. Org. Chem. USSR* **1983**, *19*, 701. (e) Rutkovskii, G. V.; Begunov, A. V.; Ignat'ev, Y. A. *Ibid.* **1983**, *19*, 710. (f) Bunton, C. A.; Gan, L.-H.; Savelli, G. *J. Phys. Chem.* **1983**, *87*, 5491. (g) Emsley, J.; Hall, D. *The Chemistry of Phosphorus*; Wiley: New York, 1976; pp 494–509. (h) Fendler, J. H.; Fendler, E. J. *Catalysis in Micellar and Micromolecular Systems*; Academic Press: New York, 1975; pp 150–161.

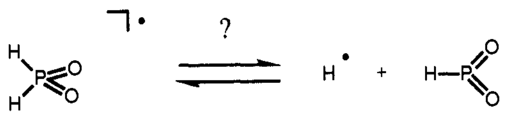

1 (C_{2v}) 2

Figure 1. Potential equilibrium between 1 and 2 + H•.

Eschirichia coli, inter alia, is capable of using organophosphonates as a sole source of phosphorus during growth.[5] Although isolation of the enzymes responsible has not yet been effected, the crucial step, cleaving the P–C bond, has been implicated to proceed via P–C homolysis in either a phosphonyl or phosphoranyl radical.[5c,d] Experiment is, however, as yet unable to select between the two. Clearly, elucidation of the exact mechanism by other methods is desirable.

The ability to probe the nature of short-lived intermediates and reaction transition states is potentially the greatest weapon in the arsenal of computational chemistry.[6] An oft-overlooked additional benefit is that neither the environment nor any researcher has yet been accidentally poisoned by computational substrates. Not entirely tongue-in-cheek, we have thus focused our efforts on applying the tools of theoretical chemistry toward a better understanding of organophosphorus radicals, with particular attention to bond making/breaking processes. Although eventual extension of gas-phase, ab initio results to biological processes is tenuous at best, the level of understanding of these processes is such that fundamental molecular information still needs to be obtained, following which more biologically focused techniques may be applied.

Computational studies of organophosphorus species have included careful investigation of the phosphorus atom's role in the stabilization of α-carbanions,[7] -carbenes,[8] and -carbocations.[9] Phosphates,[10] aminophosphines,[11] phosphondiamides,[7a] and the simple phosphorus oxyacids[12] have also been the subjects of theoretical inquiry. Much of the initial effort expended on these studies was aimed at codifying the role of phosphorus d orbitals in binding and charge stabilization; the resulting axiom was that these orbitals function primarily to polarize charge and afford better Coulombic stabilization within the molecule rather than as bonding orbitals in a more classical sense.[7,10,12]

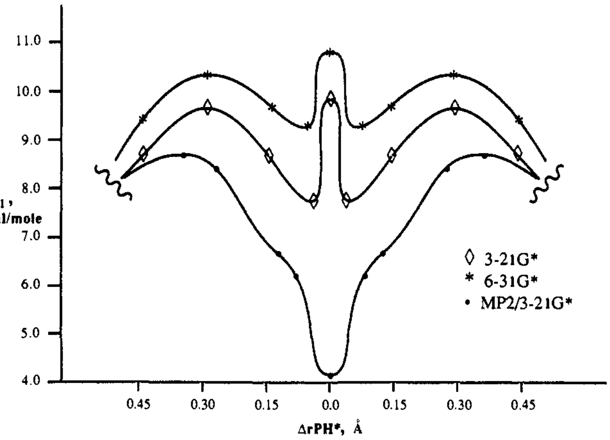

Figure 2. Relative energy vs 2 + H• as a function of P–H* bond distance for various theoretical models.

Phosphorus based radicals, on the other hand, have received comparatively little theoretical attention. Notable exceptions are the gaseous oxides PO, PO_2, and PO_3,[13] and the phosphoranyl/fluorophosphoranyl series, PH_nF_{4-n}, $n = 0$–4.[14] Given the relative paucity of theoretical data on higher homologues of these most basic species, we considered it appropriate to begin our studies with a relatively simple system, one incorporating useful symmetry properties if at all possible. The dihydrodioxophosphoranyl radical, (1, H_2PO_2) (Figure 1), nicely fits these requirements. We have examined elsewhere the likelihood of this molecule being prepared synthetically.[15] We perform here an analysis on the homolysis of a single P–H bond in 1. Our particular interests are in how basis set and electron correlation affect the theoretical description. As we intend to eventually extend these studies to relatively large *organo*phosphorus radicals, identification of a model which is both adequate and economical is our primary initial goal.

Computational Methods

All structures were fully optimized at the UHF/STO-3G(*),[16] UHF/3-21G(*),[17] UHF/6-31G*,[18] and UMP2/3-21G(*) level within the constraints of the reaction coordinate (*r*PH*) and C_s symmetry (C_{2v} for 1). Core orbitals were included in the UMP2/3-21G(*) geometry optimizations and frequency calculations, but they were frozen for single point calculations (UMP2, UMP3, CISD) at the Hartree–Fock geometries. Three- and four-point extrapolation procedures were not used in solving the SCF equation for the UMP2/3-21G(*) geometry optimizations (see Discussion). All calculations for 2 + H• were performed for the infinitely separated (10.0 Å) supermolecule to avoid CI size-consistency problems and RHF to UHF comparisons. The majority of the calculations were performed on either a Vax 11/780, microVax II, or Vaxstation 3100 using the GAUSSIAN 82[19a] package; the 6-31G* frequency

---

(5) (a) Loo, S. H.; Peters, N. K.; Frost, J. W. *Biochem. Biophys. Res. Commun.* **1987**, *148*, 148. (b) Avila, L. Z.; Loo, S. H.; Frost, J. W. *J. Am. Chem. Soc.* **1987**, *109*, 6758. (c) Frost, J. W.; Loo, S.; Cordeiro, M. L.; Li, D. *Ibid.* **1987**, *109*, 2166. (d) Cordeiro, M. L.; Pompliano, D. L.; Frost, J. W. *Ibid.* **1986**, *108*, 332.

(6) (a) Dykstra, C. E. *Ab Initio Calculation of the Structures and Properties of Molecules*; Elsevier: Amsterdam, 1988. (b) Hehre, W. J.; Radom, L.; Schleyer, P. v. R.; Pople, J. A. *Ab Initio Molecular Orbital Theory*; Wiley: New York, 1986.

(7) (a) Denmark, S. E.; Cramer, C. J. *J. Org. Chem.* **1990**, *55*, 1806. (b) Schleyer, P. v. R.; Clark, T.; Kos, A. J.; Spitznagel, G. W.; Rohde, C.; Arad, D.; Houk, K. N.; Rondan, N. G. *J. Am. Chem. Soc.* **1984**, *106*, 6467. (c) Spitznagel, G. W. Diplomarbeit, Erlangen, 1982.

(8) Nguyen, M. T.; McGinn, M. A.; Hegarty, A. F. *Inorg. Chem.* **1986**, *25*, 2185.

(9) (a) Whangbo, M. H.; Stewart, K. R. *Inorg. Chem.* **1982**, *21*, 1720. (b) Van Wazer, J. R. *Colloq. Int. C.N.R.S.* **1970**, *No. 182*, 27. (c) Hillier, I. H.; Saunders, V. R. *J. Chem. Soc. D* **1970**, 1183. (d) Marsmann, H. C.; Van Wazer, J. R.; Robert, J. B. *J. Chem. Soc. A* **1970**, 1566. (e) Bernardi, F.; Bottoni, A.; Venturini, A. *J. Am. Chem. Soc.* **1986**, *108*, 5395. (f) Wong, M. W.; Yates, B. F.; Nobes, R. H.; Radom, L. *Ibid.* **1987**, *109*, 3181.

(10) (a) Streitwieser, A., Jr.; Rajca, A.; McDowell, R. S.; Glaser, R. *J. Am. Chem. Soc.* **1987**, *109*, 4184. (b) Rajca, A.; Rice, J. E.; Streitwieser, A., Jr.; Schaefer, H. F., III *Ibid.* **1987**, *109*, 4189.

(11) Nguyen, M. T.; Hegarty, A. F. *J. Chem. Soc. Trans. 2* **1987**, 47 and references cited therein.

(12) (a) Cramer, C. J.; Dykstra, C. E.; Denmark, S. E. *Chem. Phys. Lett.* **1987**, *136*, 17. (b) Magnusson, E. *Aust. J. Chem.* **1986**, *39*, 735. (c) Magnusson, E. *Tetrahedron* **1985**, *41*, 5235. (d) Magnusson, E. *J. Comput. Chem.* **1984**, *5*, 612. (e) Schmidt, M. W.; Gordon, M. S. *Can. J. Chem.* **1985**, *63*, 1609. (f) Schmidt, M. W.; Gordon, M. S. *J. Am. Chem. Soc.* **1985**, *107*, 1922. (g) Schmidt, M. W.; Yabushita, S.; Gordon, M. S. *J. Phys. Chem.* **1984**, *88*, 382. (h) Yabushita, S.; Gordon, M. S. *Chem. Phys. Lett.* **1985**, *117*, 321. (i) Gordon, M. S.; Boatz, J. A.; Schmidt, M. W. *J. Phys. Chem.* **1984**, *88*, 2998. (j) Wallmeier, H.; Kutzelnigg, W. *J. Am. Chem. Soc.* **1979**, *101*, 2804. (k) Magnusson, E. *Aust. J. Chem.* **1985**, *38*, 23. (l) Magnusson, E. *J. Am. Chem. Soc.* **1984**, *106*, 1185. (m) Deakyne, C. A.; Allen, L. C. *J. Am. Chem. Soc.* **1976**, *98*, 4076. (n) Guest, M. F.; Hillier, I. H.; Saunders, V. R. *J. Chem. Soc. Faraday Trans. 2* **1972**, *68*, 867. (o) Hillier, I. H.; Saunders, V. R. *J. Chem. Soc. A* **1970**, 2475. (p) Van Wazer, J. R.; Marsmann, H.; Groenweghe, L. C. D.; Schaad, L. J. *J. Am. Chem. Soc.* **1970**, *92*, 6107. (q) Van Wazer, J. R. *Colloq. Int. C.N.R.S.* **1970**, *No. 182*, 27. (r) Choplin, F.; Kaufmann, G. *Bull. Soc. Chim. Fr.* **1971**, 387. (s) Archibald, R. M.; Perkins, P. G. *Rev. Roum. Chim.* **1971**, *16*, 1137.

(13) (a) Lohr, L. L.; Boehm, R. C. *J. Phys. Chem.* **1987**, *91*, 3203. (b) Lohr, L. L. *Ibid.* **1984**, *88*, 5569.

(14) (a) Demolliens, A.; Eisenstein, O.; Hiberty, P. C.; Lefour, J. M.; Ohanessian, G.; Shaik, S. S.; Velatron, F. *J. Am. Chem. Soc.* **1989**, *111*, 5623. (b) Janssen, R. A. J.; Visser, G. J.; Buck, H. M. *Ibid.* **1984**, *106*, 3429. (c) Howell, J. M.; Olsen, J. F. *Ibid.* **1976**, *98*, 7119. (d) Cramer, C. J. *J. Am. Chem. Soc.* Submitted for publication.

(15) Cramer, C. J.; Famini, G. R. *Chem. Phys. Lett.* In press.

(16) (a) Hehre, W. J.; Ditchfield, R.; Stewart, R. F.; Pople, J. A. *J. Chem. Phys.* **1970**, *52*, 2769. (b) Collins, J. B.; Schleyer, P. v. R.; Binkley, J. S.; Pople, J. A. *Ibid.* **1976**, *64*, 5412.

(17) Pietro, W. S.; Francl, M. M.; Hehre, W. J.; DeFrees, D. J.; Pople, J. A.; Binkley, J. S. *J. Am. Chem. Soc.* **1982**, *104*, 5039.

(18) Francl, M. M.; Pietro, W. J.; Hehre, W. J.; Binkley, J. S.; Gordon, M. S.; DeFrees, D. J.; Pople, J. A. *J. Chem. Phys.* **1982**, *77*, 3654.

(19) (a) Binkley, J. S.; Frisch, M. J.; DeFrees, D. J.; Raghavachari, K.; Whiteside, R. A.; Schlegel, H. B.; Fleuder, E. M.; Pople, J. A. GAUSSIAN 82 (release H version), Carnegie-Mellon University: Pittsburgh, PA, 1983. (b) Frisch, M. J.; Head-Gordon, M.; Schlegel, H. B.; Raghavachari, K.; Binkley, J. S.; Gonzalez, C.; DeFrees, D. J.; Fox, D. J.; Whiteside, R. A.; Seeger, R.; Melius, C. F.; Baker, J.; Martin, R. L.; Kahn, L. R.; Stewart, J. J. P.; Fluder, E. M.; Topiol, S.; Pople, J. A. GAUSSIAN 88; Gaussian Inc.: Pittsburgh, PA.

Table I. Relative Energies and Selected Structural Parameters for Intermediates in the P–H Bond Homolysis of **1**

model[a]	rPH*, Å	E_{rel}, kcal/mol	rPH, Å	rPO, Å	∠OPO, deg	∠HPH*, deg	nature of point[b]	structure
HF/3-21G$^{(*)}$								
	1.409	9.83	1.409	1.486	129.1	101.8	TS	**1**
	1.446	7.74	1.382	1.490	127.0	104.7	LM	**3**
	1.550	8.62	1.383	1.476	129.1	101.3	NS	
	1.694	9.61	1.381	1.458	131.2	94.5	TS	**4**
	1.850	8.66	1.379	1.449	132.0	89.0	NS	
	10.00	0.00	1.377	1.441	132.9		GM	**2** + H•
HF/6-31G*								
	1.412	10.79	1.412	1.482	130.6	104.5	TS	**1**
	1.463	9.29	1.388	1.479	130.0	105.4	LM	**3**
	1.550	9.75	1.387	1.468	131.4	102.6	NS	
	1.700	10.34	1.385	1.452	133.0	96.4	TS	**4**
	1.850	9.40	1.383	1.443	133.6	91.8	NS	
	10.00	0.00	1.381	1.435	134.2		GM	**2** + H•
MP2/3-21G$^{(*)}$								
	1.429	4.14	1.429	1.523	130.9	99.3	LM	**1**
	1.507	6.18	1.439	1.508	133.1	92.8	NS	
	1.550	6.65	1.416	1.505	132.4	92.3	NS	
	1.700	8.39	1.405	1.495	132.3	91.4	NS	
	1.774	8.65	1.403	1.491	135.7	89.3	TS	**4**
	10.00	0.00	1.398	1.483	133.4		GM	**2** + H•

[a] All structures were fully optimized at the indicated level. [b] GM, global minimum; LM, local minimum; NS, nonstationary point; TS, transition state.

Table II. Relative Energies along the P–H Reaction Coordinate at Various Levels of Theory

level	relative energy, kcal/mol					
	1	**3**	(rPH* = 1.55 Å)	**4**	(rPH* = 1.80 Å)	**2** + H•
3-21G$^{(*)}$						
HF/3-21G$^{(*)}$	9.83	7.74	8.62	9.61	8.66	0.00
MP2/3-21G$^{(*)}$//3-21G$^{(*)}$	3.30	5.11	5.58	7.71	8.00	0.00
MP3/3-21G$^{(*)}$//3-21G$^{(*)}$	0.40	1.17	2.62	6.06	7.11	0.00
CISD/3-21G$^{(*)}$//3-21G$^{(*)}$	2.28	2.39	3.64	6.50	7.23	0.00
6-31G*						
HF/6-31G*	10.79	9.29	9.75	10.34	9.40	0.00
MP2/6-31G*//6-31G*	3.26	4.55	5.23	7.34	7.79	0.00
MP2/3-21G$^{(*)}$						
MP2/3-21G$^{(*)}$//MP2/3-21G$^{(*)}$	4.14	(6.18)[a]	6.65	8.65		0.00

[a] Calculated with rPH* frozen at 1.507 Å.

calculations were performed on an Ardent Titan using the GAUSSIAN 88[19b] package.

Results

Investigation of this system focused on mapping the one-dimensional reaction coordinate corresponding to the breaking of one of the two degenerate P–H bonds in radical **1**. One general problem in the study of open-shell molecules is that the spin-unrestricted Hartree–Fock (UHF) wave functions[20] can occasionally show serious contamination from higher multiplicity spin states, especially when smaller basis sets are employed.[6] The spin-restricted open-shell Hartree–Fock formalism (ROHF)[21] has been demonstrated to give results similar or superior to those from UHF with smaller basis sets, but inferior to those from UHF with more flexible (larger) basis sets.[6] As none of the wave functions encountered here showed appreciable spin contamination (the expectation value of the total spin operator varied between 0.75 and 0.80), the UHF formalism was employed throughout.

Thus, with the P–H* bond frozen at increasing lengths, we performed complete geometry optimizations on a number of intermediates within the constraints of C_s symmetry using the three polarized basis sets STO-3G$^{(*)}$, 3-21G$^{(*)}$, and 6-31G*. As expected from the use of UHF wave functions, none of the intermediates exhibited any zwitterionic character, consistent with simple bond homolysis. Furthermore, all of the intermediates were of electronic state $^2A'$, removing some of the difficulties of studying this reaction at the single determinant HF level.

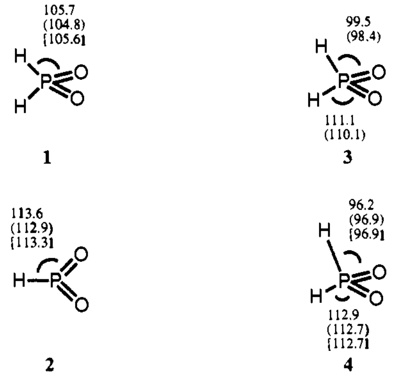

Figure 3. Structures of the four stationary points on the SCF reaction coordinate (bond angles not in Table I are presented as 3-21G$^{(*)}$ (6-31G*)[MP2/3-21G$^{(*)}$]).

Although all three basis sets examined predicted similar structures for both **1** and the closed-shell product **2**, the energies predicted by the STO-3G(*) basis were of little value as this model treats the free hydrogen atom very poorly. The failure of this basis set to reproduce electronic properties while nevertheless providing accurate structural information has been noted elsewhere.[6b] We therefore confined ourselves to the remaining two polarized, split-valence basis sets. The results are portrayed graphically in Figure 2 with electronic and structural data presented in Tables I and II.

We were somewhat surprised to find that at the HF level both basis sets predict **1** to be a transition state. Between **1** and **2** + H•, two other stationary points were located: a local minimum,

---

(20) Pople, J. A.; Nesbet, R. K. *J. Chem. Phys.* **1954**, *22*, 571.
(21) Roothan, C. C. J. *Rev. Mod. Phys.* **1960**, *32*, 179.

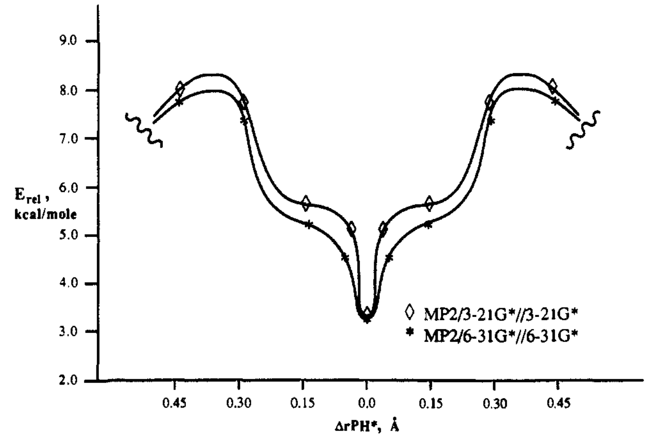

Figure 4. Relative energy vs 2 + H• as a function of P-H* bond distance for two theoretical models incorporating a second-order Møller-Plesset correction.

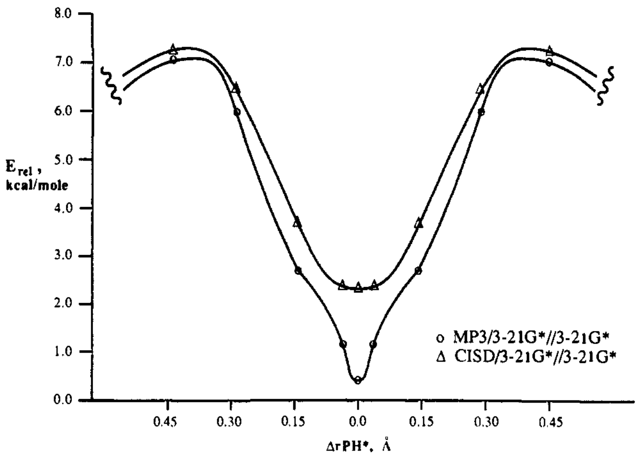

Figure 5. Relative energy vs 2 + H• as a function of P-H* bond distance for the 3-21G$^{(*)}$ model with higher level inclusion of correlation effects.

3, and a transition state for bond breaking, 4 (Figure 3). Vibrational analysis confirmed these assignments, with 1 and 4 each having a single imaginary frequency (1289i and 843i, respectively, at the 3-21G$^{(*)}$ level) and 2 and 3 each having none.

However, a number of open-shell molecules have been shown to inaccurately prefer C_s symmetric structures over those of C_{2v} symmetry as a result of Hartree-Fock doublet instability,[22] leading to just such a double-well potential as that observed here. The most notorious example is the allyl radical.[23] Inclusion of electron correlation effects is generally sufficient to resolve this phenomenon. Although configuration interaction, which directly includes higher energy microstates in the post-Hartree-Fock wave function, is generally the preferred technique for evaluating correlation energy in systems evincing doublet instability, Møller-Plesset perturbation theory truncated at second order (MP2)[24] was first investigated as it is a considerably more economical technique. Relative energies from single point calculations at the various geometries obtained from both the 3-21G$^{(*)}$ and 6-31G* levels are collected in Table II and presented graphically in Figure 4. Although the MP2 method does indicate 1 to be of lower energy than 3 for both basis sets, the energy curve generated along the reaction coordinate does not increase from 1 to 4 in the expected fashion, but rather kinks upward at 3. At the MP2/6-31G* level, this kinking is less pronounced, but it is evident nonetheless.

Third-order Møller-Plesset theory (MP3) and configuration interaction incorporating all single and double substitutions (CISD) were next investigated. Since little difference was observed at the HF and MP2 levels between the two basis sets under consideration, only the much more economical 3-21G$^{(*)}$ basis set was employed for these methods.[25] Relative energies may again be found in Table II with the results portrayed graphically in Figure 5. At the MP3/3-21G$^{(*)}$ level, the kinking of the potential curve is much less pronounced than at the MP2/3-21G$^{(*)}$ level. Nevertheless, there is still evident distortion from the classical, parabolic curve expected at the bottom of this potential well. The CISD/3-21G$^{(*)}$ energies, on the other hand, fit perfectly to such a curve, which is in accord with literature precedent.[20,21]

As a final step, we performed complete geometry optimizations on all of the intermediates at the MP2/3-21G$^{(*)}$ level (for the intermediate corresponding to 3, the P-H* bond was frozen at 1.507 Å), with the hopes that this optimization would remove the potential curve distortion observed in the single-point calculations. While no less time-consuming than the CISD computations, these calculations have the additional benefit of delivering geometries which should be closer to those of the real, as yet unobserved molecules. Additionally, a bond-breaking transition state was located explicitly with no need for interpolation on a single-point energy curve. The relative energies and structural data may be found in Table I and Figures 2 and 3.

As expected, the optimized bond lengths are up to 0.05 Å longer than those found at the HF level. Additionally, the H-P-H angle is considerably smaller at the MP2/3-31G$^{(*)}$ level for those structures on the reaction coordinate close to 1. It is evident, however, that use of MP2/3-21G$^{(*)}$ geometries does not cure the poor performance of the MP2 method at describing the potential curve near 1, it remains significantly distorted.

Discussion

Because either of the two equivalent P-H bonds in 1 may homolyze, the reaction coordinate may be viewed as corresponding to the symmetrical substitution of hydrogen in HPO_2 by another hydrogen atom. Although the reaction mechanism at the HF level is predicted to be $A_R{}^*A_RD_R{}^{**}D_R$, it is simply AR + DR at the post-HF level.[26] Supporting the assertion that HF doublet instability accounts for the discrepancy, when the wave function for the C_{2v} symmetric 1 was allowed to converge to a broken symmetry (C_s) solution, the UHF energy was lowered by nearly 20 kcal/mol. This symmetry breaking of the wave function was observed when density extrapolation techniques[27] were employed to speed convergence.[21h] Like the double-well potential, this is also a general phenomenon of doublet instability.[21]

Although UHF wave functions can exhibit stability where the corresponding ROHF do not,[21c] or acquire stability upon substitution of a larger basis set for a smaller,[21g] that is evidently not the situation here, as even at the 6-31G* level the energy difference between the C_{2v} 1 and the C_s 3 is 1.5 kcal/mol. In addition, vibrational analysis at the 6-31G* level still shows an imaginary frequency at 896i. It appears, however, that it might be possible to eliminate the instability with a very large basis set, since 6-31G* *does* represent an improvement over 3-21G$^{(*)}$, where the energy difference between 1 and 3 is 2.1 kcal/mol and the imaginary

---

(22) For a discussion of the general Hartree-Fock instability problem, see: Chambaud, G.; Levy, B.; Millie, P. *Theor. Chim. Acta* **1978**, *48*, 103.

(23) Allyl radical: (a) Benard, M.; Paldus, J. *J. Chem. Phys.* **1980**, *72*, 6546. (b) McKelvey, J.; Hehre, W. J. *Mol. Phys.* **1973**, *25*, 983. (c) Cook, D. B. *J. Chem. Soc., Faraday Trans. 2* **1986**, *82*, 187. . Formyloxyl radical: (d) McLean, A. D.; Longsfield, B. H.; Pacansky, J.; Ellinger, Y. *J. Chem. Phys.* **1985**, *83*, 3567. Imidazolyl and pyrazolyl radicals: (e) Van der Meer, K.; Mulder, J. J. C. *Tetrahedron* **1976**, *32*, 1555. (f) Bofill, J. M.; Olivella, S.; Solé, A. *J. Am. Chem. Soc.* **1989**, *111*, 7740. Homonuclear diatomics: (g) Farnell, L.; Pople, J. A.; Radom, L. *J. Phys. Chem.* **1983**, *87*, 79. Cyclopropyl radical: (h) Mezey, P. G.; Strausz, O. P.; Gosavi, R. K. *J. Comput. Chem.* **1980**, *1*, 178.

(24) Møller, C.; Plesset, M. S. *Phys. Rev.* **1934**, *46*, 618.

(25) We have previously noted the favorable comparison of the 3-21G$^{(*)}$ basis set with those near the Hartree-Fock limit in the closed-shell H_3PO system; see ref 7a.

(26) These mechanistic descriptions use the newly described IUPAC symbology: (a) Commision on Physical Organic Chemistry, IUPAC *Pure Appl. Chem.* **1989**, *61*, 23, 57. (b) Guthrie, R. D.; Jencks, W. P. *Acc. Chem. Res.* **1989**, *22*, 343.

(27) For a general reference, see: Veillard, A. In Computational Techniques in Quantum Chemistry and Molecular Physics *NATO Advanced Study Institute Series*; Reidel: Dordrecht, 1975.

Table III. Predicted Spectral Constants for **1**

IR frequency, cm^{-1} [a,b]				Fermi contact value, au[c]			rotational constants, GHz[a]	μ, D[a]	quadrupole moment, B[a]
A_1	A_2	B_1	B_2	H	O	P			
382 m	873 w	$896i$[d]	996 m	0.082	0.084	−0.219	44.85	3.078	$Q_{xx} = -21.24$[e]
722 w		2002 m	1421 s				8.35		$Q_{yy} = -32.21$[f]
917 w									$Q_{zz} = -22.48$[g]
2152 w									

[a] Calculated at the HF/6-31G*//6-31G* level. [b] Frequencies corrected using bond-type specific coefficients (see: Cramer, C. J.; Reutter, D. J.; Famini, G. R.; Duncan, D. *J. Appl. Chromatog.*, submitted for publication). [c] Calculated at the MP2/3-21G$^{(*)}$ geometry. [d] This imaginary frequency was not corrected. [e] The *x* axis was taken as perpendicular to the PO_2 fragment. [f] The *y* axis was taken as perpendicular to the PH_2 fragment. [g] The *z* axis was taken as the C_2 rotation axis.

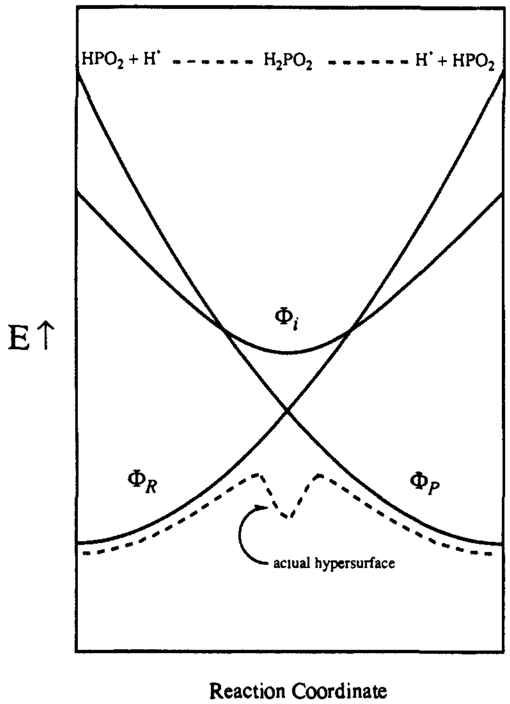

Figure 6. Curve crossing diagram illustrating qualitatively the existence of a metastable, symmetrical intermediate in the substitution reaction of hydrogen in HPO_2.

frequency is correspondingly larger.

It has been suggested that the presence of nonbonded electron pairs on atoms formally bearing significant fractions of the odd electron dramatically increases the likelihood of doublet instability being exhibited.[21f] Analysis of the Fermi contact terms in **1** indicates fairly weak spin localization on the oxygens (Table III). However, an equivalent symmetrically substituted intermediate, PH_4, has been calculated at the UHF/6-31G* level to be a weakly bound local minimum exhibiting no doublet instability (vide infra).[14a] Of course, a comparison of these two systems is hardly definitive. Calculation of the isoelectronic bis(trihydroborato)- or dimethylenedihydrophosphoranyl would provide a more critical assessment of the importance of lone pairs to this phenomenon.

The weak stability of the aforementioned, simple, tetrasubstituted phosphorus radical, PH_4, has been discussed in the context of valence bond (VB) theory. Considering the symmetrical hydrogen exchange reaction for $PH_3 + H^\bullet$ proceeding through PH_4, the stability of the tetrasubstituted radical arises from the mixing of a ($n \rightarrow \sigma^*$) configuration VB function into the reactant and product Lewis curves.[14a] This intermediate configuration, Φ_i, achieves its lowest energy, and hence mixes most efficiently, at the center point on the reaction coordinate. This point corresponds to C_{2v} PH_4 and thus to the intersection of the reactant, Φ_R, and product, Φ_P, Lewis curves. A curve crossing diagram illustrates this concept in Figure 6. Energy lowering which arises from multiple "avoided crossings" results in a symmetrical, metastable intermediate or even global minimum if Φ_i is low enough in energy. A similar analysis may be applied to **1**, where the intermediate configuration which achieves its lowest energy for **1** represents a ($n \rightarrow \pi^*$) VB function—specifically, the $1A_2 \rightarrow 3B_1$ excitation in both **1** and **2**. The lower energy of this ($n \rightarrow \pi^*$) Φ_i for **1** relative to the ($n \rightarrow \sigma^*$) Φ_i for PH_4 accounts for the roughly 4.0-kcal/mol smaller difference in the relative energies of **1** and **2** + H˙ compared to PH_4 and PH_3 + H˙.

As to the likelihood of observing **1** experimentally, if it can be synthesized,[15] we predict a barrier to homolytic decomposition of 4.8 ± 0.3 kcal/mol. Although the close relative energies of **1** and **2** + H˙ indicate that at equilibrium a sizable amount of **1** should be present, it must be pointed out that **2** is a high-energy isomer of HOPO.[13a] The barrier to unimolecular rearrangement to **2** is expected to be quite high,[7] but under conditions which allow for other than unimolecular processes, the equilibrium drain from loss of **2** would be very rapid. Hence, observation of **1** will be restricted to conditions under which only unimolecular processes occur. Generation of **1** in a suitably cold matrix, however, should allow identification of the molecule. To assist such identification, a variety of predicted electronic and spectroscopic data are collected in Table III. Although the imaginary IR frequency clearly casts some doubt on the validity of the IR data, the P–O normal modes are probably trustworthy. In addition, the negative spin density at phosphorus is particularly noteworthy.

In conclusion, it appears that the 3-21G$^{(*)}$ basis set is of adequate size for the study of phosphorus–hydrogen bond homolysis. Treatment of correlation effects via configuration interaction is required to obtain a good description of the reaction coordinate in the vicinity of the tetrasubstituted phosphorus species. Near the homolysis transition state, on the other hand, these effects are less profound.[28] The barrier to homolysis is predicted to be 4.8 ± 0.3 kcal/mol at the MP2/3-21G$^{(*)}$//3-21G$^{(*)}$, MP2/6-31G*//6-31G*, MP2/3-21G$^{(*)}$//MP2/3-21G$^{(*)}$, and CISD/3-21G$^{(*)}$//3-21G$^{(*)}$ levels. For reasons which are not clear, the MP3/3-21G$^{(*)}$//3-21G$^{(*)}$ level predicts a considerably higher barrier. It may well be that going on to fourth order in the Møller–Plesset correction would return a value in closer agreement with the majority, but this was not investigated. Further work will focus on extending these results to both organo- and nonorganophosphoranyl and phosphonyl radicals.

Acknowledgment. Funding for this work was provided under Projects 1C162622A553I and 1L161102A71A. We are grateful to Steve Lawhorne and the CRDEC Data Management Office for graciously providing Vax 11/780 time free of charge and to John Holter and Linda Stine for hardware technical assistance.

---

(28) While at first this may seem surprising, since correlation energy is a significant fraction of overall bond energy, it must be remembered that this reaction is isogyric: the total number of spin-paired electrons is conserved. In addition, as the electronic state symmetry is conserved throughout, inclusion of excited microstates via CI is less important to the description of the bond-breaking intermediates than is otherwise typical.